

# Formation kinetics of pendant arm polyamine macrocycles with copper(II)†

Peter G. Lye, Geoffrey A. Lawrance and Marcel Maeder\*

Department of Chemistry, The University of Newcastle, Callaghan, New South Wales 2308, Australia. E-mail: [chmm@cc.newcastle.edu.au](mailto:chmm@cc.newcastle.edu.au)

Received 28th March 2001, Accepted 5th June 2001

First published as an Advance Article on the web 2nd August 2001

The complexation reaction between Cu(II) and a series of cyclam analogue macrocycles with dangling primary amine groups was investigated in aqueous solution. The pH dependence of the reaction was measured between pH 0 and 5.5 covering a range of different protonation stages of the ligands. The kinetics was observed by stopped-flow measurements followed at many wavelengths. An initial second order reaction results in an intermediate which isomerises to a stable complex. The observed rate constants for the initial step varied between  $1.5 \times 10^{-2} \text{ M}^{-1} \text{ s}^{-1}$  at pH 0 and  $6.3 \times 10^5 \text{ M}^{-1} \text{ s}^{-1}$  at pH 5.3; for the secondary step the rates varied between  $2 \times 10^{-4} \text{ s}^{-1}$  at pH 1 and  $24 \text{ s}^{-1}$  at pH 5.3. The pH dependence was successfully analysed in terms of the different reactivities for differently protonated ligands for the first step and differently protonated complexes for the second step. Ligands with unprotonated dangling primary amines react with rate constants of  $10^6$ – $10^7 \text{ M}^{-1} \text{ s}^{-1}$ , the rates drop dramatically upon protonation of the arms to *ca.*  $10$ – $10^2 \text{ M}^{-1} \text{ s}^{-1}$  which are very similar to the rates of the parent cyclam ligand of equivalent protonation. The pH dependence of the secondary isomerisation reaction is explained in similar ways: protonated, dangling arms inhibit the isomerisation reaction completely.

## Introduction

The investigation of both complex formation and dissociation kinetics results in a deeper understanding of the chemistry of coordination compounds than that possible from the determination of equilibrium constants alone.<sup>1</sup> For aqueous solutions, there is a wealth of equilibrium<sup>2</sup> data available but complex formation kinetic data is relatively scarce.<sup>3</sup> Even though there has been a series of detailed investigations into the formation kinetics of labile metal ions with tetraazamacrocycles,<sup>4–7</sup> information is scarce and our understanding limited when compared to that of complexation equilibria for such systems.

The appearance of macrocyclic ligands with pendant donor groups capable of binding to metal ions *exo* to the macrocyclic cavity has raised the suggestion that the rate of complexation of the metal ion into the macrocyclic cavity may be enhanced. This idea was first described for the complexation rate of a “picket-fence” porphyrin.<sup>8</sup> The rate of metal incorporation into porphyrins is exceptionally slow, a fact that has been attributed to a weak outer-sphere association complex followed by rate determining desolvation of the metal and/or deformation of the rigid planar porphyrin framework.<sup>9</sup> However, the situation was found to be very different for the tetra-carboxylic acid “picket-fence” porphyrins. The initial step in the complexation has been reported as a rapid complexation of the metal ion ( $\text{Cu}^{2+}$ ) by the four carboxylate groups followed by the rate determining metal ion transfer from the  $\text{O}_4$  sites to the porphyrin nucleus.<sup>8</sup>

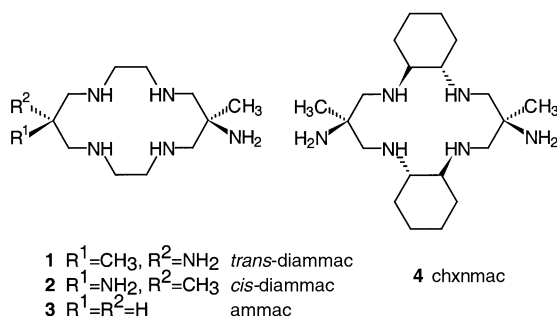
The complexation kinetics of polyaza polyacetate macrocycles has received some interest,<sup>10,11</sup> which has been inspired by their possible medical applications as contrast agents in magnetic resonance imaging (MRI)<sup>12</sup> and for labelling monoclonal antibodies.<sup>13</sup> Detailed studies have been carried out in aqueous solution, with the monoprotonated ligand species  $\text{LH}^{3-}$  found

to be the reactive ligand species over the pH range of the study (pH 5 to 9).<sup>14</sup> The general reaction mechanism for these macrocycles seems to be *via* a path similar to that described for the “picket-fence” porphyrins. There is a rapidly formed intermediate involving both a coordinating carboxylate and a ring nitrogen, which subsequently transforms with  $\text{H}^+$  release to the final product. Interestingly, the  $\text{LH}_2^{2-}$  species for the macrocycles are shown to be relatively unreactive, which has been tentatively ascribed to hydrogen bonding between an acetate arm and the tertiary nitrogen to which it is attached, therefore effectively stopping the functioning of the acetate arm in complexation with the incoming metal ion.<sup>14</sup>

The reaction of a cyclam analogue with a pendant 2,2'-bipyridin-6-yl-methyl arm has been studied with labile metal ions in DMSO solution.<sup>15</sup> Two stages were apparent in the overall reaction: an initial, rapid, second order process, followed by a much slower first order reaction. It was concluded from the study that the bipyridyl groups are able to capture metal ions rapidly, and that the rate determining step in the overall formation process is the incorporation of the metal into the macrocyclic cavity. This study shows that, although the complexation reaction is enhanced with the addition of the pendant donor group, the fact that the bipyridyl arm forms such a stable intermediate species actually retards the incorporation of the metal ion into the macrocyclic cavity. Thus, it is important to note, that when attempting to enhance complex formation rates of macrocycles by adding pendant donor groups, the pendant donors, which are the points of initial attachment, should not provide a structure of such stability that the metal ion is hindered in its movement into the macrocyclic ring.

The pendant arm macrocycles, (1)–(4), would seem to fit nicely when considering the criteria described above. The pendant primary amines on their own would hardly be expected to form strong and rigid complexes, since they can act initially as only a unidentate donor. However, these types of donor provide a point of initial attachment for a metal ion prior to its subsequent incorporation into the macrocyclic cavity. These

† Electronic supplementary information (ESI) available: initially fitted values for  $k_{1,\text{obsd}}$  and  $k_{2,\text{obsd}}$  and buffer concentration dependence of  $\log(k_{1,\text{obsd}})$  and  $\log(k_{2,\text{obsd}})$ . See <http://www.rsc.org/suppdata/dt/b1/b102845f/>



flexible macrocycles have the additional advantage of efficiently spreading the charge density in partially protonated forms. Even at relatively low pH one of the arms (in the case of (1), (2), and (4)) remains unprotonated.<sup>16,17</sup>

In this work we present a study of the complex formation kinetics of the above group of polyaza pendant arm macrocycles with the labile metal ion  $Cu^{2+}$ . In order to gain detailed understanding of the reaction, an extensive pH dependence has been carried out. The complexation reactions of polydentate ligands in aqueous solution are invariably complicated by multiple protonation equilibria of the free ligand and also of intermediate complexes. Each differently protonated form of the ligand reacts with a specific rate constant with the metal ion. As the protonation constants are often not well separated, the different forms co-exist and their individual rate constants cannot be determined independently. Only the analysis of extensive pH dependences allows the resolution of the individual rate constants  $k_{MLH_n}$ . Unfortunately, the situation is even more complicated: it is impossible to directly determine the rate for the reaction between the metal ion and the unprotonated ligand L, as at high pH the metal ions are in the form of either hydroxide precipitates or aquahydroxy complexes. The complex formation kinetics of the ligands (1)–(4) with copper hydroxo complexes at high pH has been reported recently.<sup>18</sup> The reactivities of the hydroxo complexes cannot be compared straightforwardly with those of the aqua complexes. The necessary buffering of the solutions introduces the additional complication of possible interactions of the buffer anions with either the metal ion<sup>19</sup> or polyprotonated ligand cations.<sup>20</sup>

This work may be considered an extension of other work that has been reported on the reaction of tetraazamacrocycles with a range of labile metal ions.<sup>21</sup> The ligands included in the study are shown above. Due to the presence of pendant arms, the ligands (1)–(4) may well be expected to display formation rates characteristic of both linear and macrocyclic polyamines.

## Experimental

### Chemicals and solutions

The preparation of the *trans* (1) and *cis* (2) isomers of 6,13-dimethyl-1,4,8,11-tetraazacyclotetradecane-6,13-diamine as hexachloride salts (1)·6HCl·2.5H<sub>2</sub>O and (2)·6HCl·1.5H<sub>2</sub>O have been described previously,<sup>22</sup> as has the synthesis of the pentamine 6-methyl-1,4,8,11-tetraazacyclotetradecane-6-amine (3) as the tetrachloride salt (3)·4HCl·H<sub>2</sub>O.<sup>17,23</sup> A sample of the *cis* isomer of *R,R*:*R,R*-4,15-dimethyl-2,6,13,17-tetraazatricyclo[16.4.0.0<sup>7,12</sup>]docosane-4,15-diamine as the hexachloride salt (4)·6HCl was supplied by G. Wei (University of Newcastle)<sup>17</sup> and the free base of 1,4,8,11-tetraazacyclotetradecane (cyclam) (5) was supplied by Aldrich Chemicals; both (4) and (5) were used without further purification. All metal salts used were of AR grade and were dried in a desiccator under vacuum at room temperature for twenty four hours prior to their use. All other reagents used were of analytical grade and used without further purification.

Ligand solutions were made using boiled milliporeQ water with the ionic strength adjusted to 0.5 mol dm<sup>-3</sup>, where pos-

sible, with the addition of the appropriate amount of KCl. The concentration of the ligands was generally kept in slight excess compared to that of the metal ion. Where buffering was required, the buffer concentration was maintained at 0.25 mol dm<sup>-3</sup> for all buffered solutions; acetate, chloroacetate and dichloroacetate were used as buffers. Reactions in strong acid did not require buffering and the ionic strength was maintained at 1 mol dm<sup>-3</sup> with both KCl and HCl.

The pH of all the buffered solutions was measured using a Metrohm combined glass electrode, whereas for the strong acid solutions the pH of the solution was calculated using the known acid concentrations. Between five and ten measurements were made for individual pHs over varying time bases with the mean observed rate constants reported. The errors in the observed rates are reported as the standard deviation of the  $(k_{obsd})_i$  values and thus represent the reproducibility of the individual kinetic runs.

Data analysis was performed on PCs using a non-linear least squares regression program based on published algorithms.<sup>24</sup> The program is written in the matrix based computer language MATLAB.

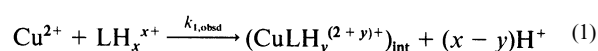
The pH dependences of the observed rate constants were fitted using the appropriate rate equations. The square sum was minimised using the molecular rate constants as parameters. Literature values for the protonation equilibrium constants were used.<sup>17,22,25,26</sup> The minimisation of the square sum was performed using the data fitting software SCIENTIST.<sup>27</sup>

### Apparatus

The complex formation kinetics of the copper(II) complexes with the polyamine macrocycles (1)–(5) were followed under second order conditions at  $298 \pm 0.1$  K with an Applied Photophysics stopped-flow spectrophotometer DX-17 MV equipped with a temperature controlled optical cell (path length = 1.0 cm). Measurements were made using the “point-by-point” method where kinetics traces are acquired individually at all the required wavelengths, which is done under complete computer control. Absorption measurements are taken at one hundred separate times and the complete collection then consists of one hundred spectra over the selected single time base, or else data sampling was done at two different time bases with fifty spectra being recorded over each time base. A tungsten lamp was used for all measurements, with suitable filters being used depending on the spectral range under study. For the slower copper(II) reactions with (1) in strong acid solutions the spectral changes were monitored on a Hitachi 220-A UV-Vis spectrophotometer, interfaced to a PC.

## Results

The formation kinetics of the macrocyclic ligands (1)–(5) have been studied with the labile metal ion copper(II). In general, two observed rates could be fitted to all of the measurements, involving a second order reaction between the metal and the ligand followed by a first order reaction. The only exceptions were the reaction of *trans*-diammac (1) with copper(II) in strongly acidic solution and also the reaction of cyclam with copper(II) in acetate buffered solution, where a single second order observed rate fitted the measurements adequately. The model that was generally used is shown below. The initial step is a second order reaction between the metal ion ( $Cu^{2+}$ ) and the differently protonated ligands ( $LH_x^{x+}$ ) with an observed rate constant  $k_{1,obsd}$ . The resultant intermediate species ( $CuLH_y^{(2+y)+}$ )<sub>int</sub> reacts in a subsequent first order reaction,  $k_{2,obsd}$ , to form the final product  $CuLH_z^{(2+z)+}$ .



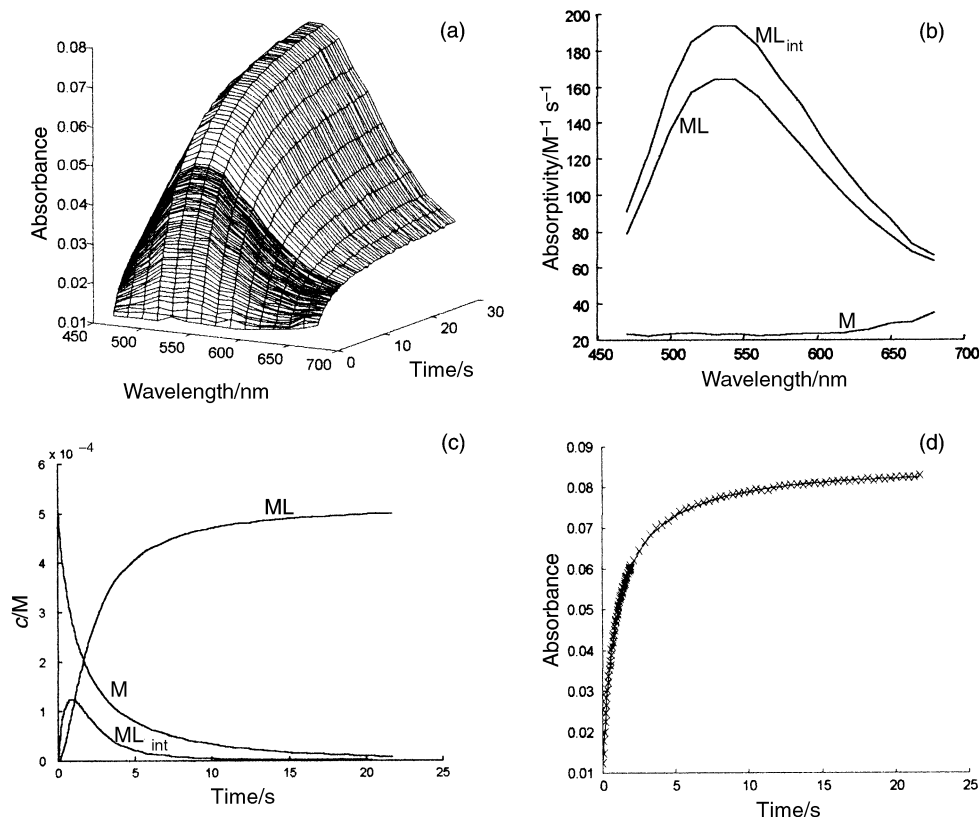


**Fig. 1** (a) Spectral changes associated with the complexation of  $\text{Cu}^{2+}$  with (1) at pH 2.85; (b) calculated spectra; (c) calculated concentration profiles; and (d) plot of measured (x) and calculated absorbance at 530 nm.

Both observed rate constants showed a distinct pH dependence. This is straightforwardly rationalised by the different degrees of protonation of  $\text{LH}_x^{x+}$  and also of the intermediate complexes  $(\text{CuLH}_y^{(2+x)+})_{\text{int}}$ .

#### Formation kinetics with *trans*-diammac

The complex formation kinetics of *trans*-diammac (1) with copper(II) has been followed over a broad pH range. Complex formation has been followed in strongly acidic solutions (pH 0–0.7), and in dichloroacetate, chloroacetate and acetate buffered solutions (pH 1.12–5.33).

A single observed rate constant was determined from the data for the complexation in strongly acidic solution. The observed rate constants are shown in Table A in the supplementary material.† No secondary step was observed at very low pH. Attempts at including the reverse dissociation reaction into the reaction model were unsuccessful, indicating that, even at these low pH values, the rate of the back reaction is negligible compared to that of the forward reaction.

Two observed rate constants ( $k_{1,\text{obsd}}$  and  $k_{2,\text{obsd}}$ ), of the form shown in eqn. (1) and (2), were fitted to the measurements made in acetate, chloroacetate and dichloroacetate buffered solutions. The fitted observed rate constants for all buffered solutions are shown in Table A (supplementary material).† Fig. 1 shows a typical measurement in chloroacetate buffered solution at pH 2.85 where the spectrum has been measured between 470 and 680 nm over a split time base with the first 50 measurements taken within 2 seconds whereas the second 50 measurements were within the next 20 seconds. Also included in Fig. 1 are the calculated spectra (b) and concentration profiles (c) for all the coloured species in addition to the comparison of the measured to calculated absorbances at 530 nm (d). The calculated spectra shown in Fig. 1(b) show that the intermediate species ( $\text{ML}_{\text{int}}$ ) has a  $\lambda_{\text{max}}$  of approximately 540 nm which is essentially the same as that for the final product (ML). The difference between the two spectra is a small decrease in the molar absorptivity for

the product. The similarity of the spectra of  $\text{ML}_{\text{int}}$  and ML strongly indicates a similar ligand environment, and the second reaction is possibly the interconversion of two isomers.

The buffer dependence of the calculated observed rate constants was studied for one example with the buffer concentration being varied between 0.15 and 0.45 mol dm<sup>-3</sup> while the pH of the solutions was maintained at 4.7. The results for the two observed rate constants are shown in Table B (supplementary material).†

#### Formation kinetics with *cis*-diammac, *cis*-chxnmac, ammac, and cyclam

The formation kinetics of ligands (2)–(5) with copper(II) have been investigated in a narrower pH range between approximately pH 2 and 5 in acetate and chloroacetate buffered solutions. Two observed rate constants,  $k_{1,\text{obsd}}$  and  $k_{2,\text{obsd}}$ , of the form shown in eqn. (1) and (2), were fitted to each of the measurements with the results shown in Table C (supplementary material).† Cyclam was fitted with only a second order reaction. These results are also collected in Table C (supplementary material).†

The calculated spectra show that the  $\lambda_{\text{max}}$  for all the intermediate species ( $\text{ML}_{\text{int}}$ ) and the final products (ML) are essentially the same, with the value near 530 nm. The molar absorptivities too are very similar, with a value of about 150 M<sup>-1</sup> cm<sup>-1</sup> for the final products. The intermediates show consistently higher molar absorptivities than the final products.

## Discussion

#### Complexation kinetics of pendant arm macrocycles with Cu(II) in aqueous acidic solution

Two sequential processes were observed for the complex formation reaction between the pendant arm macrocycles (1)–(4) and copper(II). Both observed rate constants show a very strong pH dependence. The first step is a second order reaction

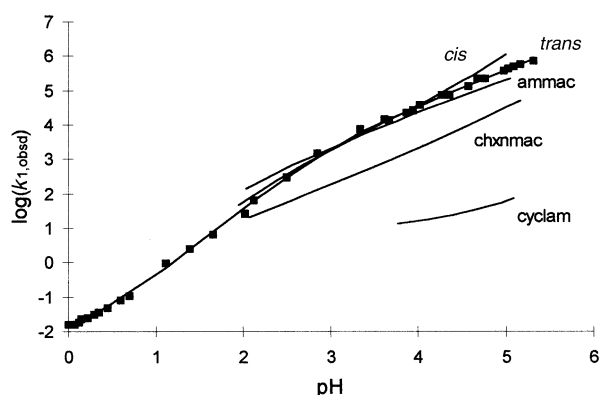
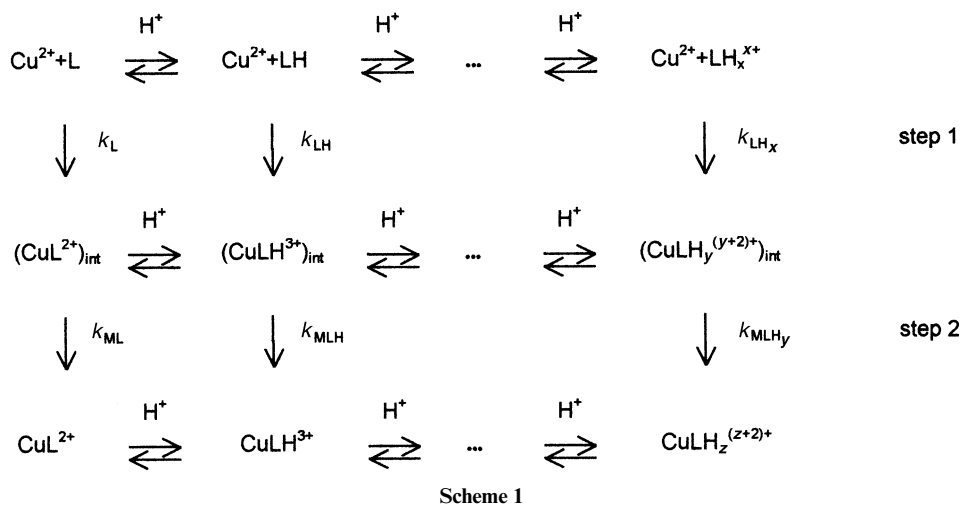


**Fig. 2** Plot of  $\log(k_{1,\text{obsd}})$  vs. pH for (1) (■) and the fitted function (solid line) based on eqn. (3). The fitted dependences for the other ligands are included in this plot without displaying the actual measurements.

between the metal ion and the ligand and thus describes the initial complex formation. Its strong pH dependence is straightforwardly explained by the different reactivities of the various protonated forms of the ligand reacting with the metal ion in the initial reaction. The second step is a first order reaction, representing the internal rearrangement of an intermediately formed complex. Here, differently protonated forms of the intermediate complex isomerize to the final product with different rates.

All the initially fitted values for  $k_{1,\text{obsd}}$  and  $k_{2,\text{obsd}}$  are collected in the Tables A–C (supplementary material).<sup>†</sup> The quantitative analyses of the pH-dependences of  $k_{1,\text{obsd}}$  and  $k_{2,\text{obsd}}$  are based on the following, general microscopic or molecular reaction pathway (Scheme 1). The differently protonated forms of the ligand react with individually different rates,  $k_{\text{LH}_x}$ , with  $\text{Cu}^{2+}$ . The intermediately formed complexes, again, co-exist in a second fast protonation equilibrium. Each of the differently protonated intermediate complexes reacts with an individual rate to form the final product. Naturally, this product is expected to display a similar protonation equilibrium.

#### Second order reaction $\text{Cu}^{2+} + \text{LH}_x^{x+} \rightarrow (\text{CuLH}_y^{(y+2)+})_{\text{int}}$

The rate constant  $k_{1,\text{obsd}}$  is quantitatively described as a function of the ligand deprotonation constants  $K_x$  ( $K_x = [\text{LH}_{x-1}][\text{H}^+]/[\text{LH}_x]$ ) and the individual rate constants  $k_{\text{LH}_x}$  in eqn. (3).

The equation includes all protonation stages of  $\text{LH}_2$  up to  $\text{LH}_5$ . Within the pH range investigated, the concentrations of

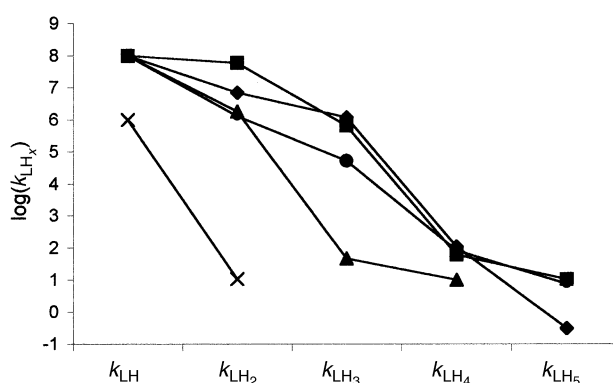


**Fig. 3** The rates  $k_{\text{LH}_x}$  for the differently protonated ligand species  $\text{LH}_x^{x+}$  with  $\text{Cu}^{2+}$ . (1) (◆), (2) (■), (3) (▲), (4) (●), and (5) (X).

**Table 1**  $\text{p}K_{\text{a}}$  values for the ligands (1) to (5)

$\text{p}K_{\text{a}}$	(1) <sup>a</sup>	(2) <sup>a</sup>	(3) <sup>b</sup>	(4) <sup>c</sup>	(5) <sup>d</sup>
$\text{p}K_1$	11.01	10.62	11.57	10.9	11.5
$\text{p}K_2$	9.96	9.68	10.22	9.6	10.3
$\text{p}K_3$	6.24	6.26	5.89	6.3	—
$\text{p}K_4$	5.52	5.40	—	5.4	—
$\text{p}K_5$	1.5	2.7	—	2.0	—

<sup>a</sup> Ref. 25. <sup>b</sup> Ref. 22. <sup>c</sup> Ref. 17. <sup>d</sup> Ref. 26.

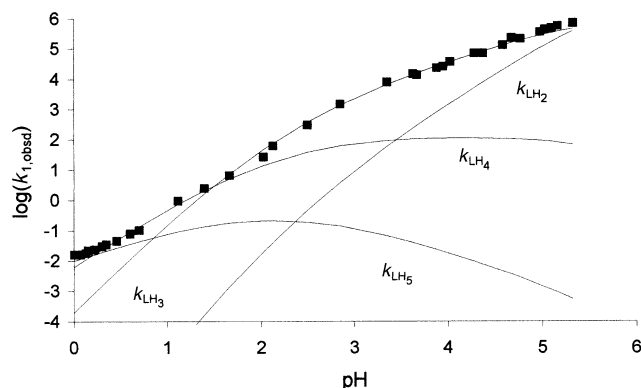
L and LH are far too low to play an observable role in the complex formation reaction. The ligands (1), (2), and (4) are potentially protonated up to  $\text{LH}_6$  but the  $\text{p}K_6$  value for this last protonation is too low and  $\text{LH}_6$  does not exist to any appreciable amount in the pH range investigated in this study. Based on the known deprotonation constants (see Table 1), the molecular rate constants  $k_{\text{LH}_x}$  are fitted to the measured  $k_{1,\text{obsd}}$  values using a standard non-linear least-squares routine. The resulting values are collected in Table 2. Fig. 2 displays the individually determined  $k_{1,\text{obsd}}$  values for (1) together with the fitted pH dependencies for all investigated ligands. The quality of the fit for the ligands (2)–(5) is similar to the quality for ligand (1) as displayed in Fig. 2.

Fig. 3 represents these results graphically. It shows clearly two different levels of reactivities: fast reactions with rate constants of  $10^6$ – $10^8 \text{ M}^{-1} \text{ s}^{-1}$  and slow reactions with rate constants in the order of  $10^1$ – $10^2 \text{ M}^{-1} \text{ s}^{-1}$ . The relationship between these two types of reactivities and the number of pendant arms is apparent: for the two-armed ligands (1), (2), and (4) the reaction is

$$k_{1,\text{obsd}} = \frac{k_{\text{LH}_2}K_3K_4K_5[\text{H}^+]^2 + k_{\text{LH}_3}K_4K_5[\text{H}^+]^3 + k_{\text{LH}_4}K_5[\text{H}^+]^4 + k_{\text{LH}_5}[\text{H}^+]^5}{K_3K_4K_5[\text{H}^+]^2 + K_4K_5[\text{H}^+]^3 + K_5[\text{H}^+]^4 + [\text{H}^+]^5} \quad (3)$$

**Table 2** Rate constants  $k_{\text{LH}_i}$  ( $\text{M}^{-1} \text{s}^{-1}$ ) for the first step in the complexation of the macrocycles (1)–(5) with copper(II)

$k_{\text{LH}_i}/\text{M}^{-1} \text{s}^{-1}$	(1)	(2)	(3)	(4)	(5)
$k_{\text{LH}}$	—	—	—	—	$(1.0 \pm 0.1) \times 10^6$
$k_{\text{LH}_2}$	$(7.1 \pm 1.0) \times 10^6$	$(5.9 \pm 0.5) \times 10^7$	$(1.8 \pm 0.1) \times 10^6$	$(1.3 \pm 0.1) \times 10^6$	$(1.1 \pm 0.1) \times 10^1$
$k_{\text{LH}_3}$	$(1.2 \pm 0.1) \times 10^6$	$(6.6 \pm 0.4) \times 10^5$	$(4.7 \pm 2.2) \times 10^1$	$(5.3 \pm 0.3) \times 10^4$	—
$k_{\text{LH}_4}$	$(1.1 \pm 0.1) \times 10^2$	$(6.2 \pm 3.4) \times 10^1$	$\approx 1.0 \times 10^1$	$(8.5 \pm 3.5) \times 10^1$	—
$k_{\text{LH}_5}$	$(3.2 \pm 0.59) \times 10^{-1}$	$\approx 10.5$	—	$\approx 7.6$	—

**Fig. 4** The logarithm of individual contributions by the different protonated ligand species ( $k_{\text{LH}_i} \times [\text{LH}_i]/[\text{L}]_{\text{tot}}$ ) of (1) to the observed rate constant  $k_{1,\text{obsd}}$  given by the markers.

fast for  $\text{LH}_2$  and  $\text{LH}_3^{3+}$ , for one-armed (3) it is fast up to  $\text{LH}_2^{2+}$  and for cyclam only up to  $\text{LH}^+$ . The protonation is most probably occurring in the following sequence: the first 2 protons are attached to the macrocyclic ring, the next 2 (1 in the case of (3)) to the pendant arms and the following protons to the ring again. Thus, the macrocycles react fast as long as there is at least one of the pendant arms free or unprotonated; this is the case up to  $\text{LH}_2$  of (3) and  $\text{LH}_3$  of (1), (2), and (4). After the next protonation, the reaction has to proceed *via* one of the unprotonated secondary ring nitrogens. This reaction is, for steric and electrostatic reasons, much slower.

Eqn. (3) can be rearranged to show the contribution of the differently protonated species to the overall observed rate  $k_{1,\text{obsd}}$ . This equation differentiates the observed rates as the sum of the individual ligand species rate constants multiplied by their relative concentrations.

$$k_{1,\text{obsd}} = k_{\text{LH}_2} \frac{[\text{LH}_2]}{[\text{L}]_{\text{tot}}} + k_{\text{LH}_3} \frac{[\text{LH}_3]}{[\text{L}]_{\text{tot}}} + k_{\text{LH}_4} \frac{[\text{LH}_4]}{[\text{L}]_{\text{tot}}} + k_{\text{LH}_5} \frac{[\text{LH}_5]}{[\text{L}]_{\text{tot}}} \quad (4)$$

The plot of each term in eqn. (4) against pH displays a clear picture of the individual rate contributions to the observed rate. Fig. 4 shows this analysis for (1), in which it can be seen that  $\text{LH}_3^{3+}$  is the dominant ligand species over the pH range from 1.5 to 5, with  $\text{LH}_2^{2+}$  contributing at high pH. The main contributions from  $\text{LH}_4^{4+}$  is observed from pH 1.5 down to about pH 0 and the main contribution from  $\text{LH}_5^{5+}$  is at negative pH values. The contributions of  $\text{LH}$  and  $\text{L}$  are insignificant; their values cannot be determined in aqueous solution.

We start the discussion of the rate constants with those for cyclam (5), as these form the basis for the comparison with those for the pendant arm macrocycles (1)–(4). The values of  $k_{\text{LH}}$  and  $k_{\text{LH}_2}$  determined for (5) ( $1.0 \times 10^6$  and  $11 \text{ M}^{-1} \text{s}^{-1}$ ) compare well with those previously reported  $5.3 \times 10^6$  and  $8.1 \text{ M}^{-1} \text{s}^{-1}$  respectively) where  $\text{Cu}(\text{CH}_3\text{COO})^+$  was considered as the reactive metal species.<sup>28</sup> In a subsequent investigation<sup>5</sup> the acetate independent rate constants ( $k_{\text{LH}}$   $(1.8 \pm 0.2) \times 10^6$  and  $k_{\text{LH}_2}$   $(0.39 \pm 0.03) \text{ M}^{-1} \text{s}^{-1}$ ) were obtained either by extrapolating to zero acetate concentration or correcting the observed rate constant by the amount to which acetate increased the rate. Whereas the rate constants for the  $\text{LH}$  species are in good agreement, the same cannot be said for the  $\text{LH}_2$  species.

The rate for the cyclam diprotonated species is vastly reduced from that for the monoprotonated species. This has previously been attributed to increased electrostatic repulsion due to the increased charge density in the macrocyclic cavity.<sup>5</sup> However, the rate constants calculated for the diprotonated ligand species for the pendant arm macrocycles (1)–(4) are faster than for cyclam by a factor of between  $10^5$  and  $10^6$ . Thus, electrostatic repulsion cannot serve as the main reason for the decrease of the formation rate constant from  $\text{LH}^+$  to  $\text{LH}_2^{2+}$ .

There is a surprising similarity between the reaction rates for the pendant arm macrocycles with those for linear polyamines. These results for  $\text{LH}_2^{2+}$  ( $10^6$ – $10^7 \text{ M}^{-1} \text{s}^{-1}$ ) are readily compared to the rate constants for the diprotonated species of the linear polyamines tetraethylene pentaamine, tetren ( $4.2 \times 10^7 \text{ M}^{-1} \text{s}^{-1}$ ),<sup>29</sup> triethylenetetramine, trien ( $7 \times 10^6 \text{ M}^{-1} \text{s}^{-1}$ )<sup>30</sup> and 2,2',2''-triaminotriethylamine, tren ( $3.8 \times 10^6 \text{ M}^{-1} \text{s}^{-1}$ ).<sup>30</sup>

The rate constants observed for the triprotonated ligand species  $\text{LH}_3^{3+}$  ( $10^5$ – $10^6 \text{ M}^{-1} \text{s}^{-1}$ ) for (1), (2) and (4) are surprisingly high for such highly charged macrocyclic ligand species. The rate for  $k_{\text{LH}_3}$  of tetren is comparable at  $1.55 \times 10^5 \text{ M}^{-1} \text{s}^{-1}$ , so this shows that the macrocycles (1), (2) and (4) are still able to react at rates similar to those for linear polyamines of the same protonation. It is notable that the rate calculated for the  $\text{LH}_3^{3+}$  ligand species of (3) alone shows a drop of a factor of  $4 \times 10^4$  when compared to that for the  $\text{LH}_2^{2+}$  species.

The rate constants for the tetraprotonated ligand species of (1), (2) and (4) and the triprotonated ligand species of (3) show significantly reduced rate constants when compared to those for  $k_{\text{LH}_3}$  and  $k_{\text{LH}_2}$  respectively. The fourth protonation of (1), (2) and (4) (third protonation of (3)) involve the protonation of the second (or for (3), only) pendant amine. Thus, the complete protonation of the pendant amines in the macrocycles (1)–(4) results in a dramatic drop in formation rate constants.

If the values of  $k_{\text{LH}_i}$  for (1) and (2) ( $k_{\text{LH}_i}$  for (3)) are compared to  $k_{\text{LH}_i}$  for cyclam, it can be seen that the rates for the pendant arm macrocycles are still faster than that for the roughly equivalent cyclam species. This is surprising considering that there is a charge difference of 2+. The further protonation of (1), (2) and (4) beyond  $\text{LH}_3^{3+}$  and (3) beyond  $\text{LH}_2^{2+}$  leaves all pendant primary amine(s) protonated. Nevertheless, although significantly reduced from those for the less protonated ligand species, these rate constants are surprisingly high when considering the electrostatic forces that must be overcome. Presently no convincing argument can be brought forward to explain this observation, except to point out that the protonated pendant amine may be displaced well away from the macrocycle cavity that would then behave like the cyclam  $\text{LH}_2^{2+}$  species. The similar rates support this view.

#### Buffer concentration dependence

Unfortunately, buffers are unavoidable in the investigation of pH dependences of complex formation reactions. Buffer anions are always potential ligands and thus interfere with the reaction under investigation. It is very difficult to find buffers which cover a wide pH range from pH 1 to 5.5 and which are non- or only weakly-coordinating ligands.<sup>19</sup>

The results of a very limited investigation into the buffer concentration dependence of both reaction rates are shown in Fig. A (supplementary material)† for acetate buffer at pH 4.7. It is clear that there is no significant effect on the observed rate

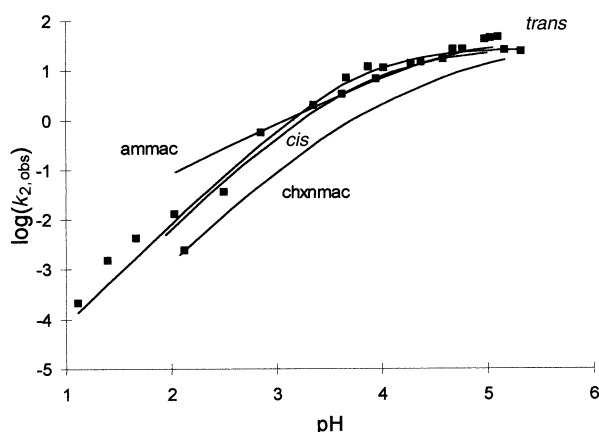


**Fig. 5** Plot of  $k_{2,\text{obsd}}$  vs. pH for (1) (■) and the fitted function (solid line) based on eqn. (5). The fitted dependences for the other ligands are included in this plot without displaying the actual measurements.

constants from variation in concentration of the acetate buffer, although it must be noted that even at  $0.15 \text{ mol dm}^{-3}$  acetate there is still a significant amount of  $\text{Cu}(\text{CH}_3\text{COO})^+$  and even  $\text{Cu}(\text{CH}_3\text{COO})_2$  present.<sup>2</sup> Additionally, there seems to be no significant effect on the observed rate in changing the buffer from acetate to chloroacetate, dichloroacetate and no buffer, as is shown in Fig. 2, where three different buffers are used and finally at low pH where the solutions are not externally buffered. From our results it is not possible to assign the reactivity to any of the different possible complexes of Cu(II) with the different buffer anions.

The influence of buffers on the reactions of metal ions with polyprotonated ligand ions is very complex and very difficult to ultimately resolve. Due to the relatively high concentration of buffer required, the copper(II) is present in part as a mixture of  $\text{Cu}^{2+}$ ,  $\text{Cu}(\text{CH}_3\text{COO})^+$  and  $\text{Cu}(\text{CH}_3\text{COO})_2$ . Of these copper(II) species, it has been reported that  $\text{Cu}(\text{CH}_3\text{COO})^+$  is the reactive metal ion species.<sup>31</sup> It was concluded in the same study that the rate constants calculated for the complexation of  $\text{Cu}(\text{CH}_3\text{COOH})^+$  with a number of monoprotonated tetraazamacrocycles are the same as those calculated for the complexation of  $\text{Cu}^{2+}_{\text{aq}}$  with the same ligands.<sup>28,32</sup> However, the situation was found to change when the diprotonated ligand  $\text{LH}_2^{2+}$  was considered with the  $\text{Cu}(\text{CH}_3\text{COO})^+$  species reacting a factor of  $10^2$  faster than that of  $\text{Cu}^{2+}_{\text{aq}}$ . In addition to the complexation of the metal cations by the buffer anions, the buffer anions are also interacting with the polyprotonated ligand cations.<sup>20</sup> This interaction is expected to be particularly strong with polyanionic buffers.<sup>19</sup>

#### First order reaction $(\text{MLH})_{\text{int}} \rightarrow \text{MLH}_2$

The pH dependences of  $k_{2,\text{obsd}}$  for (1)–(4) are listed in Tables A and C (supplementary material)† and represented in Fig. 5. Note that the errors for the determination of the individual rate constants for the second step are considerably higher than the errors for the initial reaction. Comparing Fig. 2 and 5 reveals the difference graphically. The increased inaccuracy is due to the fact that the spectral changes observed for this step are much smaller than for the first step, see also Fig. 1.

$$k_{2,\text{obsd}} = \frac{k_{\text{ML}_{\text{int}}} K_1 K_2}{K_1 K_2 + K_2 [\text{H}^+] + [\text{H}^+]^2} \quad (5)$$

(for (3):  $k_{2,\text{obsd}} = \frac{k_{\text{ML}_{\text{int}}} K_1}{K_1 + [\text{H}^+]}$ )

The pH-dependence of the reaction is similar for all ligands: we observe a limiting maximum rate which is reached at around pH 5–6. The observed rate drops off at lower pH. The slope of the pH-dependence reaches a value of 2 for the ligands (1), (2), and (4), whereas the slope for (3) is only 1.

**Table 3** Rate constant  $k_{\text{ML}}$  ( $\text{s}^{-1}$ ) for the second step and the deprotonation constants of the intermediate complex in the complexation of the macrocycles (1)–(4) with copper(II) at  $298 \pm 0.1 \text{ K}$

	(1)	(2)	(3)	(4)
$k_{\text{ML}_{\text{int}}} (\text{s}^{-1})$	$38 \pm 5$	$35 \pm 6$	$71 \pm 20$	$33 \pm 3$
$\text{p}K_1$	$4.4 \pm 0.1$	$4.4 \pm 0.1$	$5.0 \pm 0.1$	$5.1 \pm 0.1$
$\text{p}K_2$	$3.3 \pm 0.1$	$3.4 \pm 0.1$	—	$3.3 \pm 0.1$

These results are interpreted by the following mechanism. Throughout the observed pH range, the reactivity of the intermediate complex is solely due to the reaction of unprotonated complex  $(\text{CuL}^{2+})_{\text{int}}$  (Scheme 1). The contributions of the protonated forms of the intermediate complex are negligible and these rates are thus not accessible. Upon protonation at lower pH, the observed rate constant decreases according to diminishing concentration of  $(\text{ML})_{\text{int}}$ . The observed slope of 2 for the ligands (1), (2), and (4) indicates two consecutive protonations, (3) is only protonated once. These results indicate the involvement of the deprotonated pendant arms in the isomerisation step. Most probably, the protonation occurs at the pendant arms which results in the very effective suppression of the second step.

Fitting the appropriate function delivers the rate constants  $k_{\text{ML}}$  and the corresponding protonation constants, which are listed in Table 3.

#### Absorption spectra of intermediates and final products

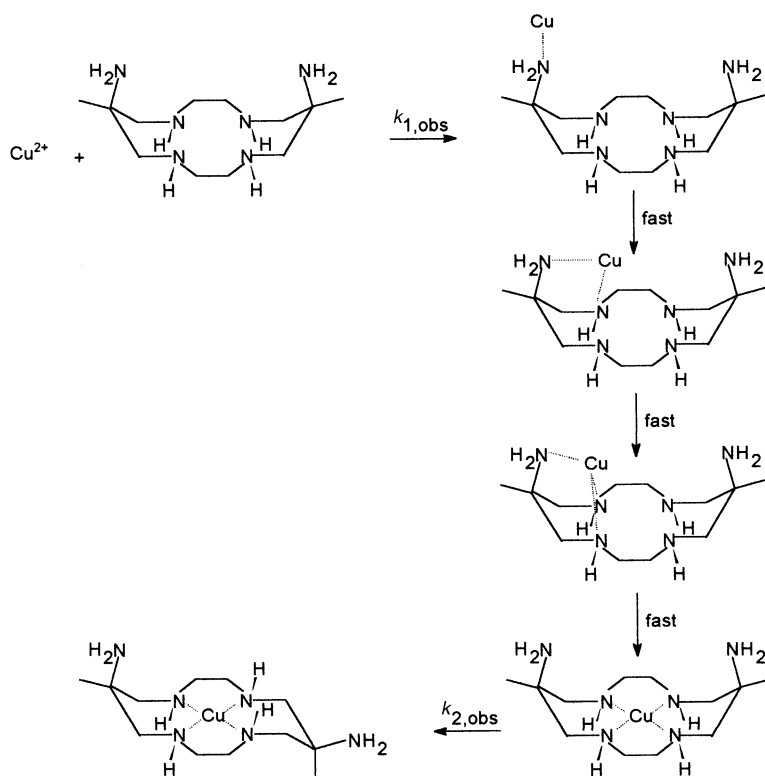
Analysis of the multiwavelength measurements allows the determination of the spectra for the intermediate and final products. The spectra for all species are characteristic of a  $\text{CuN}_4$  chromophore with absorption maxima around 530–540 nm. For all ligands there is only a small but significant drop in the absorptivity from  $\text{ML}_{\text{int}}$  to the final product ML.

#### Proposed reaction mechanism

The central result of the present investigation is the crucial involvement of unprotonated pendant amines as the initial second order step in the complex formation reaction between the metal and partially protonated ligands. It is surprising that the rates for triply protonated ligands (1), (2), and (4) are comparable to those of open chain ligands with similar degree of protonation or monoprotonated cyclam ( $k_{\text{LH}_2} \approx 10^7 \text{ M}^{-1} \text{ s}^{-1}$ ). As soon as all available pendant amines are protonated the rate constants drop dramatically by typically 4 orders of magnitude, refer to Fig. 3 and Table 2. This dramatic effect clearly cannot be attributed to the additional positive charge on the ligand. The average drop in the rate upon a simple additional protonation is only in the order of a factor of ten. The first step in Scheme 2 reflects these conclusions, it is a second order reaction between the copper ion and an unprotonated primary amine group.

The following three fast steps in Scheme 2 are not based on the present kinetic investigation, these steps are too fast to be observed. The chain of intermediates is a speculative adaptation of the results of an X-ray structure of Hg(II) complexes of (1).<sup>16</sup> Two distinct complexes were observed in the unit cell. One complex shows the mercury(II) bound to only one pendant primary amine and the second has the Hg(II) bound by a pendant primary amine and one of the secondary ring nitrogens. These exocyclic complexes are kinetically not observable. The spectrum of the intermediate indicates that it is a macrocyclic complex with a structure similar to the final product.

The second observed step most likely is an intramolecular isomerisation within a  $\text{CuN}_4$  chromophore. The small spectral changes observed for this process and also the first order rate law support this interpretation. This is indicated as the second slow step in Scheme 2.



Scheme 2

The fact that the complexes of the ligands (1), (2) and (4) can be protonated twice while the complex of (3) is protonated once only supports the structures in Scheme 2 with two unprotonated dangling primary amines. Their protonation prevents the interconversion. The observed  $pK$  values of 3 to 5 are consistent with such an interpretation. Thus, the coordination of the primary amines strongly accelerates the isomerisation reaction. Most likely, it is an N-based inversion with the secondary ring nitrogens in the intermediate in the *trans*-I configuration whereas the final products are in the *trans*-III configuration.

Secondary steps, after initial coordination, have been observed for a number of different macrocyclic ligands with Cu(II) and Ni(II) in both aqueous and non-aqueous media.<sup>6,33,34</sup> However, comparison with the rate constants determined here is difficult due to the very varied ligand structures which have been reported and the significant variation between the first and second steps. Nevertheless, N-based isomerisations are commonly involved as steps in macrocycle complexation.

## References

- 1 R. Winkler-Oswatitsch and M. Eigen, *Angew. Chem., Int. Ed. Engl.*, 1979, **18**, 20.
- 2 A. E. Martell and R. M. Smith, *Critical Stability Constants*, Plenum Press, New York, 1977, vol. 3.
- 3 R. M. Izatt, K. Pawlak and J. S. Bradshaw, *Chem. Rev.*, 1995, **95**, 2529.
- 4 D. W. Margerum, G. R. Cayley, D. C. Weatherburn and G. K. Pagenkopf, in *Coordination Chemistry*, ed. A. E. Martell, American Chemical Society, Washington, D.C., 1978, p. 1.
- 5 A. P. Leugger, C. Hertli and T. A. Kaden, *Helv. Chim. Acta*, 1978, **61**, 2296.
- 6 L. F. Lindoy, *The Chemistry of Macrocyclic Ligand Complexes*, Cambridge University Press, Melbourne, Australia, 1989.
- 7 J. R. Röper and H. Elias, *Inorg. Chem.*, 1991, **31**, 1202; J. R. Röper and H. Elias, *Inorg. Chem.*, 1991, **31**, 1210.
- 8 D. A. Buckingham, C. R. Clark and W. S. Webley, *J. Chem. Soc., Chem. Commun.*, 1981, 192.
- 9 W. Schneider, *Struct. Bonding (Berlin)*, 1975, **23**, 123; P. Hambright, in *Porphyrins and Metalloporphyrins*, ed. K. M. Smith, Elsevier, Amsterdam, 1976, ch. 6; F. Longo, in *The Porphyrins*, ed. D. Dolphin, Academic Press, New York, 1978, vol. 5, ch. 10.
- 10 E. Brucher and A. D. Sherry, *Inorg. Chem.*, 1990, **25**, 1555.
- 11 X. Wang, T. Jin, V. Comblin, A. Lopez-Mut, E. Merciny and J. F. Desreux, *Inorg. Chem.*, 1992, **31**, 1095.
- 12 R. B. Lauffer, *Chem. Rev.*, 1987, **87**, 901; Y. Liu and C. Wu, *Pure Appl. Chem.*, 1991, **63**, 427.
- 13 D. Parker, *Chem. Br.*, 1990, **26**, 942; T. A. Kaden, *Nachr. Chem. Tech. Lab.*, 1990, **38**, 728.
- 14 S. P. Kasprzyk and R. G. Wilkins, *Inorg. Chem.*, 1982, **21**, 3349.
- 15 F. McLaren, P. Moore and A. M. Wynn, *J. Chem. Soc., Chem. Commun.*, 1989, 798.
- 16 P. G. Lye, G. A. Lawrance, M. Maeder, B. W. Skelton, H. Wen and A. H. White, *J. Chem. Soc., Dalton Trans.*, 1994, 793.
- 17 G. Wei, M. Maeder and G. A. Lawrance, *Polyhedron*, 1996, **15**, 3157.
- 18 P. G. Lye, G. A. Lawrance and M. Maeder, *Inorg. React. Mech.*, 1999, **1**, 153.
- 19 A. Kandegedara and D. B. Rorabacher, *Anal. Chem.*, 1999, **71**, 3140.
- 20 M. G. Basallote, J. Durán, M. J. Fernández-Trujillo, M. A. Mañez and B. Szpoganicz, *J. Chem. Soc., Dalton Trans.*, 1999, 1093.
- 21 H. Elias, *Coord. Chem. Rev.*, 1999, **187**, 37.
- 22 P. G. Lye, PhD Dissertation, University of Newcastle, 1995.
- 23 G. A. Lawrance, M. Rossignoli, B. W. Skelton and A. H. White, *Aust. J. Chem.*, 1987, **40**, 1441.
- 24 M. Maeder and A. D. Zuberbühler, *Anal. Chem.*, 1990, **62**, 2220.
- 25 M. Micheloni, A. Sabatini and P. Paoletti, *J. Chem. Soc., Perkin Trans. 2*, 1978, 828; M. Micheloni, P. Paoletti and A. Vacca, *J. Chem. Soc., Perkin Trans. 2*, 1978, 945.
- 26 Y. Baran, G. A. Lawrance and E. W. Wilkes, *Polyhedron*, 1997, **16**, 599.
- 27 Micromath Scientist, Version 2.0, Micromath, Salt Lake City, Utah, USA, 1995.
- 28 M. Kodama and E. Kimura, *J. Chem. Soc., Dalton Trans.*, 1977, 1423.
- 29 R. E. Shepherd, G. M. Hodgson and D. W. Margerum, *Inorg. Chem.*, 1971, **10**, 989.
- 30 T. S. Roche and R. G. Wilkins, *J. Am. Chem. Soc.*, 1974, **96**, 5082.
- 31 M. Kodama and E. Kimura, *J. Chem. Soc., Dalton Trans.*, 1978, 104.
- 32 M. Kodama and E. Kimura, *J. Chem. Soc., Dalton Trans.*, 1976, 1720.
- 33 W. Steinmann and T. A. Kaden, *Helv. Chim. Acta*, 1975, **58**, 1358.
- 34 B.-F. Liang, D. W. Margerum and C.-S. Chung, *Inorg. Chem.*, 1979, **18**, 2001.